DOI：10.19789/j.1004-9398.2022.04.005
文献引用：韩超，龙文．边缺陷诱导的双层锯齿型石墨烯纳米带能隙[J]．首都师范大学学报（自然科学版），2022，43（4）：23-32+45. HAN C，LONG W. Edge-defect induced gaps in zigzag bilayer graphene nanoribbons[J]. Journal of Capital Normal University（Natural Science Edition），2022，43（4）：23-32+45.

边缺陷诱导的双层锯齿型石墨烯纳米带能隙*

韩　超，龙　文**

（首都师范大学物理系，北京　100048）

摘要：双层锯齿型石墨烯纳米带无能隙，不利于设计石墨烯场效应晶体管，边界线缺陷可打开能隙，使双边占据格点波函数变为单边占据，为设计双层石墨烯纳米器件提供理论支持．本文利用紧束缚模型，计算了双层锯齿型石墨烯纳米带能谱和格点波函数．数值计算表明，边界线缺陷层间跃迁可打开AA堆叠能隙，边界线缺陷占位能可打开AB堆叠能隙．双层锯齿型石墨烯纳米带的弱局域化行为与单层不同，缺陷占位能和层间跃迁可分别使双边占据的波函数变为单边占据，适当的缺陷占位能可使电子在上层（或下层）呈现优势占据．利用非平衡格林函数方法，研究了两端口有限尺寸双层锯齿型石墨烯纳米带的电子输运，计算了有边界线缺陷时体系的局域态密度和透射概率．

关键词：紧束缚模型；锯齿型；双层石墨烯纳米带；边态；能谱
中图分类号：O411

Edge-defect induced gaps in zigzag bilayer graphene nanoribbons*

HAN Chao，LONG Wen**

（Department of Physics，Capital Normal University，Beijing　100048）

Abstract：Zigzag bilayer graphene nanoribbons are gapless，which is not good at the design of graphene field effect transistors. The edge line defects can open the band gap and the edge state localized on both sides may be tuned on one side，which provides theoretical support for the design of bilayer graphene nanodevices. The energy spectrum and lattice wave function of bilayer zigzag graphene nanoribbons are calculated by using the tight-binding model. The numerical results show that the hopping between edge line defects can open the AA stacking gap，and the on-site energy of edge line defects can open the AB stacking gap. The weak localization behavior in the bilayer zigzag graphene nanoribbons is different from that of single layer. The defect on-site energy and interlayer hopping can change the localized edge state，respectively. Appropriate defect on-site energy can make the electrons dominant in the upper layer（or lower layer）. The electron transport of two-terminal bilayer zigzag graphene nanoribbons was investigated by using the non-equilibrium Green's function method，and the local state density and transmission probability of the system with edge defect were calculated.

收稿日期：2021-11-26
* 国家自然科学基金面上项目（11074174）
** 通信作者：longwen@cun.edu.cn

Keywords:tight-binding model;zigzag;bilayer graphene nanoribbons;edge state;energy spectrum
CLC:O411

0 引 言

2004年,英国曼彻斯特大学物理和天文学系教授Novoselov等[1]用机械剥离方法成功制备出了石墨烯,并于2010年获得了诺贝尔物理学奖.石墨烯晶格由2个不等价子格构成,导带和价带在2个不等价的Dirac点以圆锥形相切[2-3],这2个Dirac点手性相反,组成一个时间反演对,这使得二维石墨烯具有独特的电子特性[4-8],如具有半整数量子霍尔效应[9],没有背散射[10]等.石墨烯独特的电子结构使得其可以通过栅压[11]、磁场调控[12-14]、化学掺杂[15]和边缘缺陷[16]修饰其性能.

双层石墨烯[17-21]是由2层石墨烯经范德华力耦合在一起,每层含2个子格,分别称为A子格和B子格,通常有2种堆叠形式,AA和AB堆叠(即伯纳尔形式堆叠).双层石墨烯在许多方面表现出与单层石墨烯截然不同的性质,如量子霍尔效应[14,17]、边态[22]、弱局域态[23]、无序[24]和最小电导率[25-26]以及其他有趣现象[27-29].通过外加电场[30-31]等方式可以连续调整零能量点附近的带隙,改变电荷密度分布[17],诱导低密度铁磁性[32].

当顶层石墨烯相对于底层石墨烯层旋转一定角度时会形成转角石墨烯,可显著改变双层石墨烯的电子能带.转角石墨烯所具有的扭转自由度进一步丰富了双层石墨烯的物理性质,使转角石墨烯成为探索电子奇特性质[33-37]、光学[38-41]以及范德华异质结构热行为[42-43]的重要元件.转角石墨烯的一个显著例子是魔角,即其以一个小扭角(如1.08°)错位,在费米能级附近具有平带[33,35,37].最近的实验已经证实,这些扭角诱导的平带,产生了非常规的超导性[33]以及相关(莫特)绝缘状态[34].这些发现激发了大量的理论和实验工作,试图阐明魔角石墨烯潜在的物理性质和应用[35,38-39,44-50].转角石墨烯可以作为高阶拓扑绝缘体的有力候选材料[48].

石墨烯纳米带是一种新型量子线,既可看作是条带状小尺寸的石墨烯,也可看作是纵向切割碳纳米管的产物,是一种新型的准一维碳纳米材料[51-53].因其特殊的边缘限域效应,使石墨烯纳米带比石墨烯更灵活可控[54],较高长宽比的结构特点使得电子在石墨烯纳米带中的横向移动受限,从而只能纵向移动导致其具有半导体的性能[55-56].研究表明,石墨烯纳米带的边缘构型、宽度和层数对其电学性能、磁学性质和化学性质等产生决定性影响[57-58].因此,石墨烯纳米带是一种极具应用潜力的新型纳米材料.

双层石墨烯纳米带是由单层石墨烯纳米带通过一定的堆叠方式形成的准三维结构系统,包括AA和AB堆叠.类似地,用纳米带的边界形状来定义双层石墨烯纳米带,即分为锯齿型和扶手型.不考虑电子自旋时,扶手型纳米带的电子特性和纳米带的宽度有关,宽度为$3n+2$时,体系呈金属性,其余呈半导体性;而锯齿型纳米带的能带在费米面附近简并,体系只呈金属性[3,59-60],这在一定程度上限制了双层锯齿型石墨烯纳米带在量子器件中的应用.

边缘态因其独特的物理性质,在介观输运中十分重要,这使得边缘态在固态电子学二维系统中成为研究的一个热点.改变纳米带边态能量[61-63]以及边缘无序[64]均会对石墨烯纳米带能带结构产生影响.对于锯齿型石墨烯纳米带而言,局域态一直存在于Dirac点附近.因此,锯齿型石墨烯纳米带体现出类金属行为,这些特性与传统的半导体量子线的性质十分不同,这就为裁制输运和光学性质的石墨烯纳米带提供了可能[65].因此,本文主要利用无相互作用的紧束缚模型,研究边界线缺陷对双层锯齿型石墨烯纳米带能谱及边态的影响.

1 模型和公式

双层锯齿型石墨烯纳米带堆叠类型和含线缺陷的单胞如图1所示.t_0是层内最近邻原子间相互作用,t_1是上层A原子与垂直下层B原子间的层间相互作用,t_2是上层六角中心B原子与下层最近邻A原子间的层间相互作用,t_3和t_4分别是A原子间和B原子间的最近邻层间相互作用.本文统一使用蓝色表示上层,黑色表示下层.带宽沿X方向分为N层,每层含一个锯齿链,有2类格点原子,一类位于A格点,另一类位于B格点.每个单胞含$4N$个格点,纳米带沿Y方向具有周期平移不变性.

考虑如图1(c)和(d)所示的单胞,并让其两端向两侧沿Y方向无限延伸[66-67].含边界线缺陷的无

限长锯齿型双层石墨烯纳米带满足的等效差分方程为

$$\left(E\boldsymbol{I}-\boldsymbol{H}_{00}\right)\boldsymbol{\Phi}_j=\boldsymbol{H}_{01}\boldsymbol{\Phi}_{j+1}+\boldsymbol{H}_{01}^{+}\boldsymbol{\Phi}_{j-1},\qquad(1)$$

式中

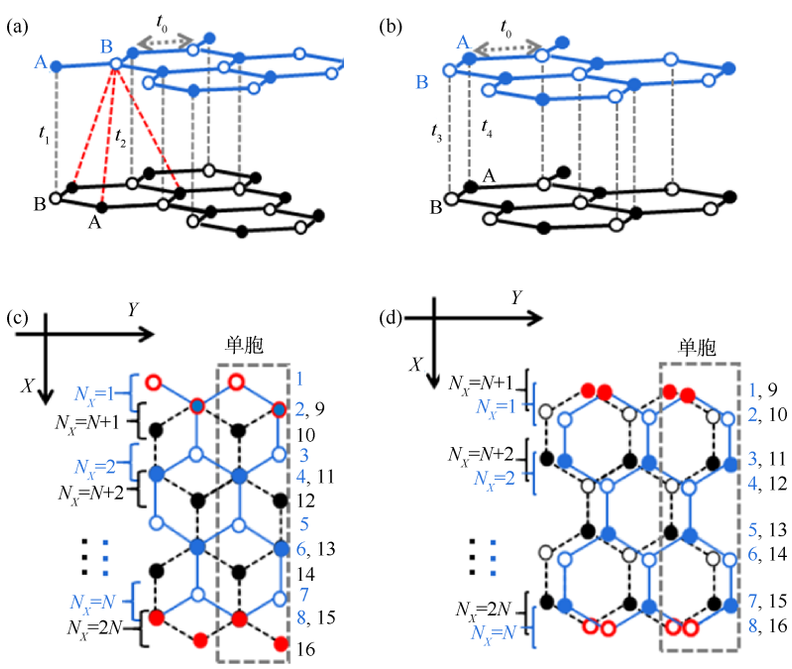
$$\boldsymbol{\Phi}_j=\left(\Phi_{j1},\Phi_{j2},\Phi_{j3}\cdots\Phi_{j4N_X}\right)^{\mathrm{T}}\qquad(2)$$

是双层锯齿型石墨烯纳米带的单胞格点波函数,T 表示转置,E 表示电子能量,$\boldsymbol{H}_{00}$ 和 $\boldsymbol{H}_{01}$ 分别表示占位能矩阵和交叠积分矩阵,$\boldsymbol{I}$ 为单位矩阵,这 3 个矩阵都是 $4N\times4N$ 的.利用双层锯齿型石墨烯纳米带沿 Y 方向具有平移不变性,考虑到波函数具有 Bloch 波形式,可将式(1)改写为

$$\left(E\boldsymbol{I}-\boldsymbol{H}_{00}\right)\boldsymbol{\Phi}_j=\boldsymbol{H}_{01}\mathrm{e}^{\mathrm{i}k_Ya}\boldsymbol{\Phi}_j+\boldsymbol{H}_{01}^{+}\mathrm{e}^{-\mathrm{i}k_Ya}\boldsymbol{\Phi}_j,\qquad(3)$$

式中 $a=0.246$ nm 是石墨烯的晶格常数.求解上述等效差分方程可得到双层锯齿型石墨烯纳米带的能带结构和能量本征波函数.

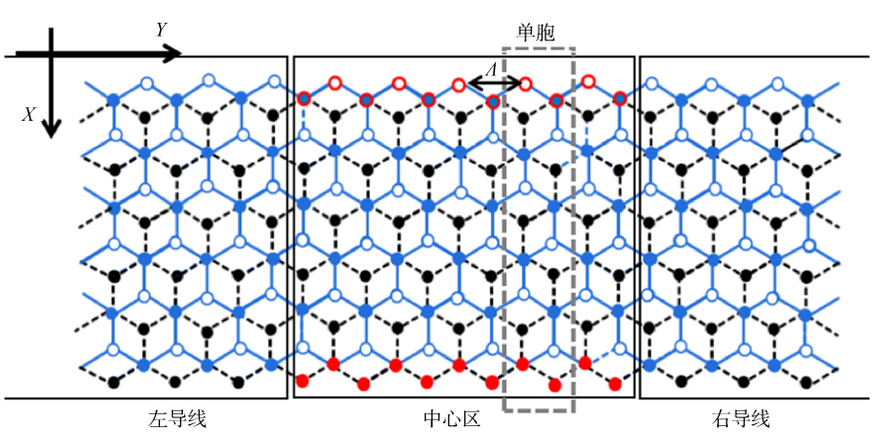
考虑一个含双层锯齿型石墨烯纳米带的量子输运系统,如耦合到左、右导线的含缺陷 AB 堆叠双层锯齿型石墨烯带(图 2).在最近邻紧束缚模型近似下,体系的总哈密顿量为



注:蓝色和黑色数字分别表示单胞上层和下层格点编号;实点表示 A 子格;空点表示 B 子格;红色表示缺陷.

图 1　双层锯齿型石墨烯层间相互作用及单胞

(a)AB 堆叠;(b)AA 堆叠;(c)AB 堆叠含边界线缺陷时的单胞;(d)AA 堆叠含边界线缺陷时的单胞



注:Λ 代表相邻单胞间距;实点代表 A 原子;空点代表 B 原子.

图 2　耦合到左、右导线的含缺陷 AB 堆叠双层锯齿型石墨烯带

$$\boldsymbol{H}=\boldsymbol{H}_{\text{中心区}}+\boldsymbol{H}_{\text{导线}}+\boldsymbol{H}_{\text{耦合}},\tag{4}$$

式中:第1项$\boldsymbol{H}_{\text{中心区}}$表示中心区AB堆叠含缺陷双层锯齿型石墨烯纳米带哈密顿量,在紧束缚近似下可表示为

$$\boldsymbol{H}_{\text{中心区}}=\sum_{l,i,j}\left(\varepsilon_{l,i}a_{l,i}^{+}a_{l,i}+\varepsilon_{l,j}b_{l,j}^{+}b_{l,j}\right)-t_0\sum_{l,<i,j>}\left(a_{l,i}^{+}b_{l,j}+\text{h.c.}\right)-t_1\sum_{<i,j>}\left(a_{1,i}^{+}b_{2,j}+\text{h.c.}\right)-t_2\sum_{<i,j>}\left(b_{1,i}^{+}a_{2,j}+\text{h.c.}\right),\tag{5}$$

式中:$a_{l,i}^{+}\left(b_{l,j}^{+}\right)$和$a_{l,i}\left(b_{l,j}\right)$分别是$l$层中A(B)子格格点上的产生算符和湮灭算符,其中$l=1,2$表示双层石墨烯的上、下层;$\varepsilon_{l,i}$表示$l$层$i$格点占位能,正常格点的占位能$\varepsilon_0=0$,平衡态费米能为0;$\sum_{<i,j>}$表示对最近邻格点求和;h.c.表示厄密共轭项;取层内正常格点间的交叠积分$t_0=3.160\,\text{eV}$为能量单位;AB堆叠中,上层A原子到垂直下层B原子的跃迁交叠积分为$t_1=0.390\,\text{eV}$;上层六角形中心B原子到下层A原子的跃迁交叠积分为$t_2=0.315\,\text{eV}$[64].AA堆叠中,上层A(B)原子到下层A(B)原子的跃迁交叠积分$t_3=t_4=0.400\,\text{eV}$,带宽$N=10$.本文用$u_{l,\text{A}}(u_{l,\text{B}})$表示各层中上(下)边界线缺陷格点占位能系数(缺陷的占位能等于占位能系数乘以正常值),$t_{\text{A}}(t_{\text{B}})$表示上(下)边界线缺陷层间跃迁系数(缺陷的层间跃迁值等于跃迁系数乘以正常值).式(4)中的第2项表示半无限长左、右导线哈密顿量,其表达式类似于式(5),所有参数取正常值;式(4)中的第3项表示中心区与左、右导线的耦合哈密顿量,中心区的边界格点与左、右导线通过耦合常数τ_{L}和τ_{R}直接耦合.

在格林函数范式下,双层锯齿型石墨烯纳米带的透射概率为

$$T=\text{Tr}\left[\boldsymbol{\Gamma}_{\text{L}}\boldsymbol{G}^{\text{r}}_{\text{中心区}}\boldsymbol{\Gamma}_{\text{R}}\boldsymbol{G}^{\text{a}}_{\text{中心区}}\right],\tag{6}$$

式中:$\boldsymbol{\Gamma}_{\text{L}}$和$\boldsymbol{\Gamma}_{\text{R}}$分别表示左、右导线的耦合矩阵,$\boldsymbol{G}^{\text{r}}_{\text{中心区}}$和$\boldsymbol{G}^{\text{a}}_{\text{中心区}}$分别表示中心输运区的延迟格林函数和超前格林函数.中心输运区能量为E的电子格林函数为

$$\boldsymbol{G}^{\text{r}}_{\text{中心区}}=\left[\boldsymbol{G}^{\text{a}}_{\text{中心区}}\right]^{+}=\left[(E+\text{i}\eta)\boldsymbol{I}-\boldsymbol{H}_{\text{中心区}}-\boldsymbol{\Sigma}^{\text{r}}_{\text{L}}-\boldsymbol{\Sigma}^{\text{r}}_{\text{R}}\right]^{-1},\tag{7}$$

式中:$\eta\to0^{+}$,$\boldsymbol{I}$为单位矩阵,$\boldsymbol{\Sigma}^{\text{r}}_{\text{L}}$和$\boldsymbol{\Sigma}^{\text{r}}_{\text{R}}$分别表示中心区与左、右导线耦合的延迟自能.

体系的局域态密度(ρ_{DOS})为

$$\rho_{\text{DOS}}=\frac{1}{2\pi}\text{Tr}\left[\boldsymbol{G}^{\text{r}}_{\text{中心区}}\left(\boldsymbol{\Gamma}_{\text{L}}+\boldsymbol{\Gamma}_{\text{R}}\right)\boldsymbol{G}^{\text{a}}_{\text{中心区}}\right].\tag{8}$$

2　计算与讨论

本文研究2种堆叠类型的双层锯齿型石墨烯纳米带的能带结构、导带底单胞格点波函数、透射概率和局域态密度.

2.1　AA堆叠双层锯齿型石墨烯纳米带

AA堆叠双层锯齿型石墨烯纳米带的能带结构如图3所示.首先分析边界线缺陷对能带结构的影响.由于层间原子A(B)-A(B)之间的跃迁势,打破了单层石墨烯的空间对称性,使得其能带二重简并被解除,能带分裂成4条,能带分裂的程度是上下2层间A(B)-A(B)之间的跃迁能.$t_{\text{A}}(t_{\text{B}})$表示上(下)边界线缺陷层间跃迁系数,$u_{l,\text{A}}(u_{l,\text{B}})$表示各层上(下)边界线缺陷格点占位能系数.当只改变体系上边界A子格的层间跃迁系数,且设定t_{A}=−15,则次价带顶和次导带底平带部分的色散关系会改变,在费米面附近打开一个能隙;当改变层间跃迁系数的同时改变边界线缺陷的占位能系数,即设定$u_{1,\text{A}}=u_{1,\text{B}}=-0.3$,$u_{2,\text{A}}=u_{2,\text{B}}=0.3$,可知4条平带的色散关系均可以被改变;当继续增大占位能系数绝对值,即设定$u_{1,\text{A}}=u_{1,\text{B}}=-0.8$,$u_{2,\text{A}}=u_{2,\text{B}}=0.8$,导带底和价带顶平带部分更加远离费米面,弯曲程度增大.由此可知,通过改变边界线缺陷的层间跃迁值,能够打开AA堆叠双层锯齿形石墨烯纳米带的一个能隙,并且如果同时改变合适的占位能,会增大能隙的宽度,能隙的宽度受占位能严格调控.

AA堆叠双层锯齿型石墨烯纳米带导带底单胞格点波函数模随纵向波矢的演化如图4所示.本文给出了导带底的单胞格点波函数的模与波矢k_Y的具体关系,每一种条件展示3个波矢,每幅图中各小图从上到下依次表示波矢$k_Y=0.67\pi$、0.80π和0.90π,X轴为单胞格点位置.无缺陷时,当k_Y从0.67π(Dirac点附近)到π时,电子逐渐占据边态,当$k_Y=\pi$时,电子完全占据边态.而如果改变边界层间跃迁值时,会使电子呈现单边占据;当占位能绝对值较大时,电子边态占据不明显,基本呈现均匀分布.并且,本文研究了导带底和价带顶波函数分布情况,显示在无缺陷和只改变边界层间跃迁时,导带底和价带顶的波函数分布情况是一致的,而如果改变占位能后,即设定占位能符号相反时,导带底和价带顶的波函数分布情况会呈现上层和下层相反的特点.由此可

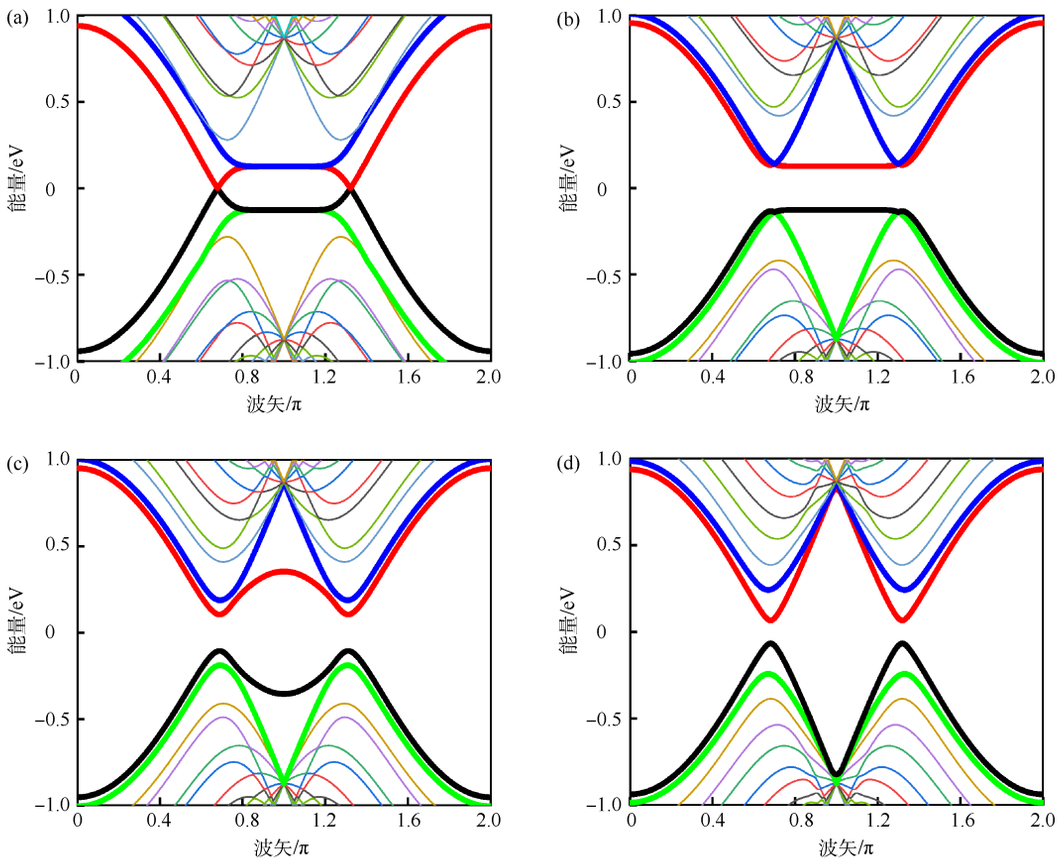


图 3　AA 堆叠双层锯齿型石墨烯纳米带的能带结构

(a)无缺陷;(b)t_A =− 15.0;(c)t_A =− 15.0,t_B = 1.5,$u_{1,A}$ = $u_{1,B}$ =− 0.3, $u_{2,A}$ = $u_{2,B}$ = 0.3;
(d)t_A =− 15.0,t_B = 1.5,$u_{1,A}$ = $u_{1,B}$ =− 0.8, $u_{2,A}$ = $u_{2,B}$ = 0.8

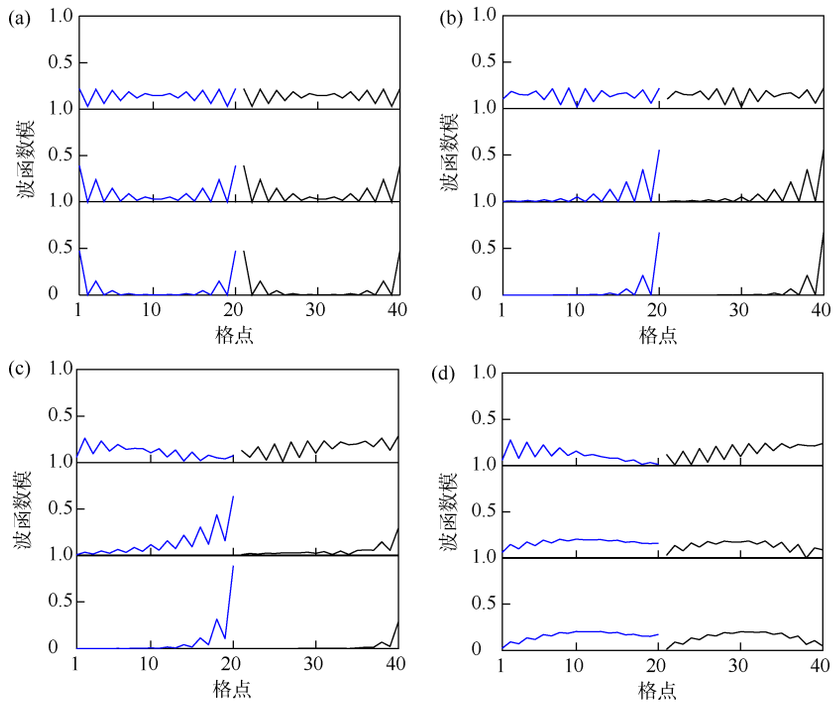
知,边界层间跃迁和占位能数值会影响电子边态占据,但当占位能较大时对边态影响不大,同时,占位能还会影响电子在上层或下层的分布情况,这取决于上层或下层占位能的符号.

AA 堆叠双层锯齿型石墨烯纳米带透射概率和局域态密度如图 5 所示.对于无缺陷情况而言,AA 堆叠双层锯齿型石墨烯纳米带在 E=0 附近的局域态密度产生了尖峰,这主要是因为费米面附近平带的作用,因为体系横向子带的受限,可以在透射概率分布图上观察到平台.当改变层间跃迁系数或者同时改变层间跃迁系数和占位能系数,透射概率和局域态密度在 E=0 附近的范围内为 0,说明此时对应的重合能带被打开.

2.2　AB 堆叠双层锯齿型石墨烯纳米带

AB 堆叠双层锯齿型石墨烯纳米带的能带结构如图 6 所示.首先分析边界线缺陷对能带结构的影响,无缺陷 AB 堆叠双层锯齿形石墨烯能带结构与单层锯齿型石墨烯纳米带的能带结构相似,只是 AB 堆叠的双层锯齿形石墨烯纳米带能带在费米面附近存在 4 条无能隙模连接导带和价带,即在费米面附近存在 4 条平带;通过改变体系边界占位能,设上层上边界 A 子格和下边界 B 子格占位能系数为 $u_{1,A}$ = $u_{1,B}$ =− 0.5, 下层上边界 A 子格和下边界 B 子格占位能系数为 $u_{2,A}$ = $u_{2,B}$ = 0.5,在费米面附近打开 1 个能隙,但此时能隙的值较小;当上层和下层上边界 A 子格线缺陷占位能系数为 $u_{1,A}$ = $u_{2,A}$ =− 0.3,上层和下层的下边界线缺陷 B 子格占位能系数为 $u_{1,B}$ = $u_{2,B}$ = 0.3,打开的能隙宽度较之前增大;继续增大占位能系数,当 $u_{1,A}$ = $u_{2,A}$ =− 0.8, $u_{1,B}$ = $u_{2,B}$ = 0.8 时,平带的弯曲程度较之前增大,说明边界线缺陷占位能影响费米面附近平带部分的弯曲程度,且费米面附近打开的能隙宽度也增大.由此可知,边界线缺陷的占位能会改变费米面附近能带的弯曲程度,并且通过改变合适的占位能符号和数值,可以在费米面附近打开能隙,能隙的宽度受占位能绝对值影响.

AB 堆叠双层锯齿型石墨烯纳米带导带底单胞格点波函数模随纵向波矢的演化如图 7 所示.本文

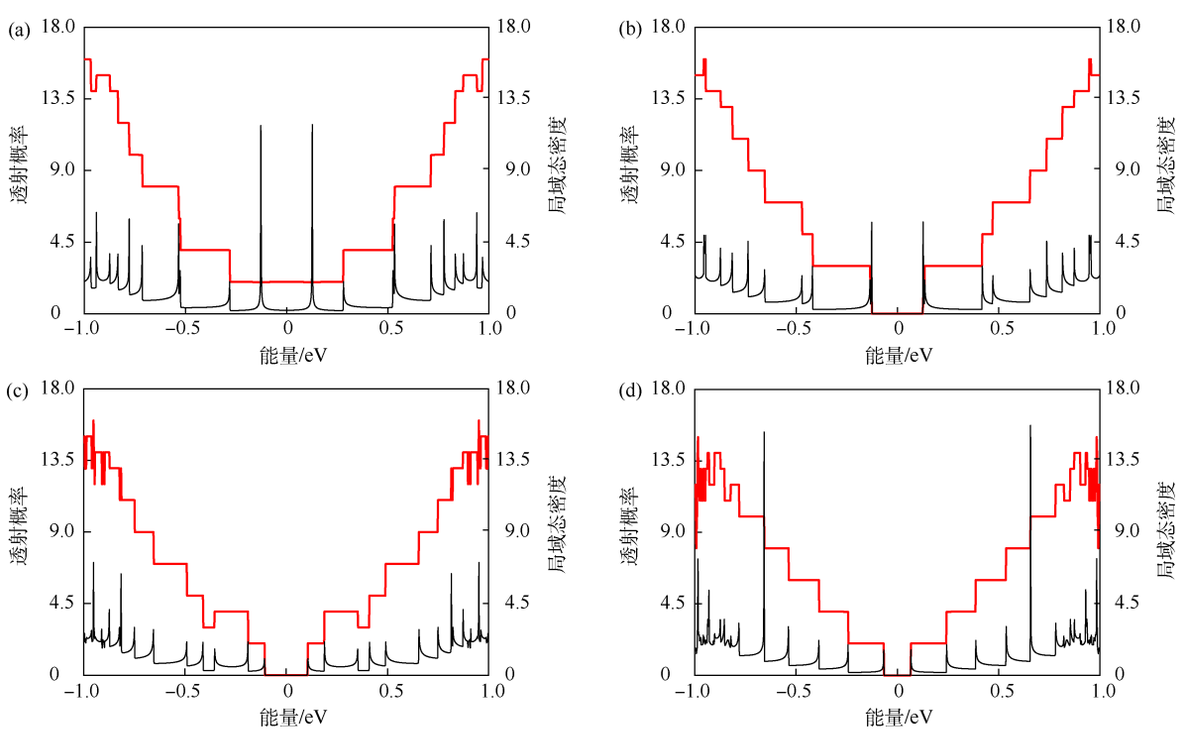


注:蓝色代表上层格点;黑色代表下层格点.

图4　AA堆叠双层锯齿型石墨烯纳米带导带底单胞格点波函数模随纵向波矢的演化

(a)无缺陷;(b)t_A =- 15.0;(c)t_A =- 15.0,t_B = 1.5,$u_{1,A}$ = $u_{1,B}$ =- 0.3,$u_{2,A}$ = $u_{2,B}$ = 0.3;

(d)t_A =- 15.0,t_B = 1.5,$u_{1,A}$ = $u_{1,B}$ =- 0.8,$u_{2,A}$ = $u_{2,B}$ = 0.8



注:红粗实线表示透射概率;黑细实线表示局域态密度.

图5　AA堆叠双层锯齿型石墨烯纳米带透射概率和局域态密度

(a)无缺陷;(b)t_A =- 15.0;(c)t_A =- 15.0,t_B = 1.5,$u_{1,A}$ = $u_{1,B}$ =- 0.3,$u_{2,A}$ = $u_{2,B}$ = 0.3;

(d)t_A =- 15.0,t_B = 1.5,$u_{1,A}$ = $u_{1,B}$ =- 0.8,$u_{2,A}$ = $u_{2,B}$ = 0.8

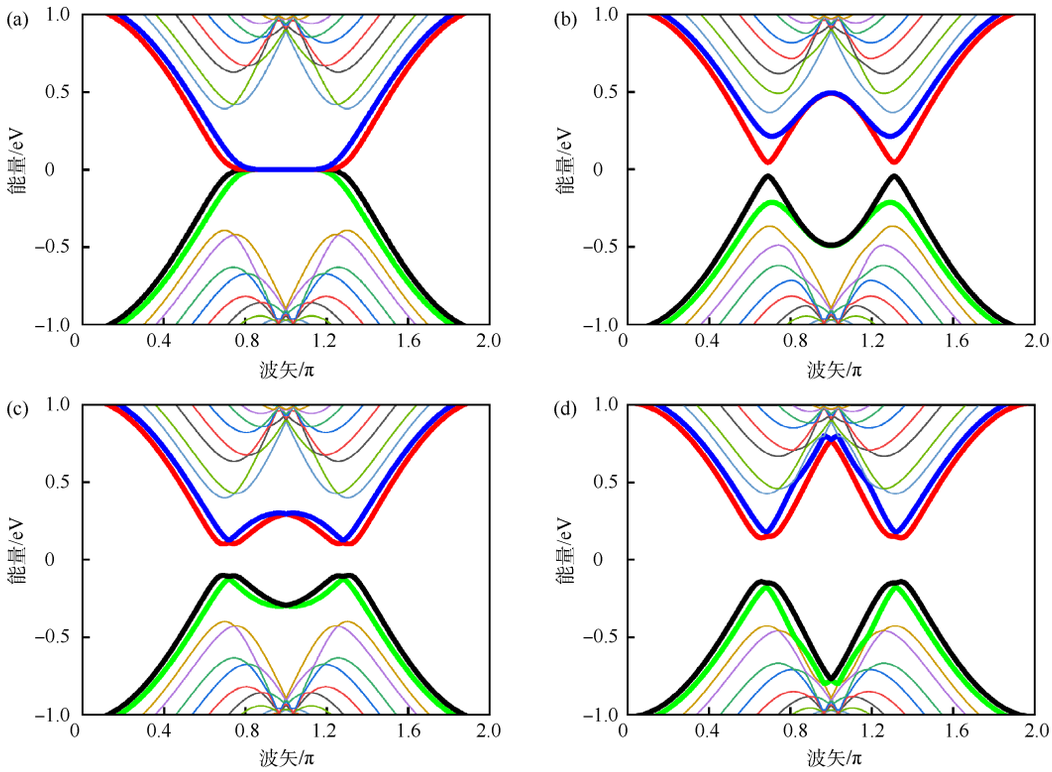
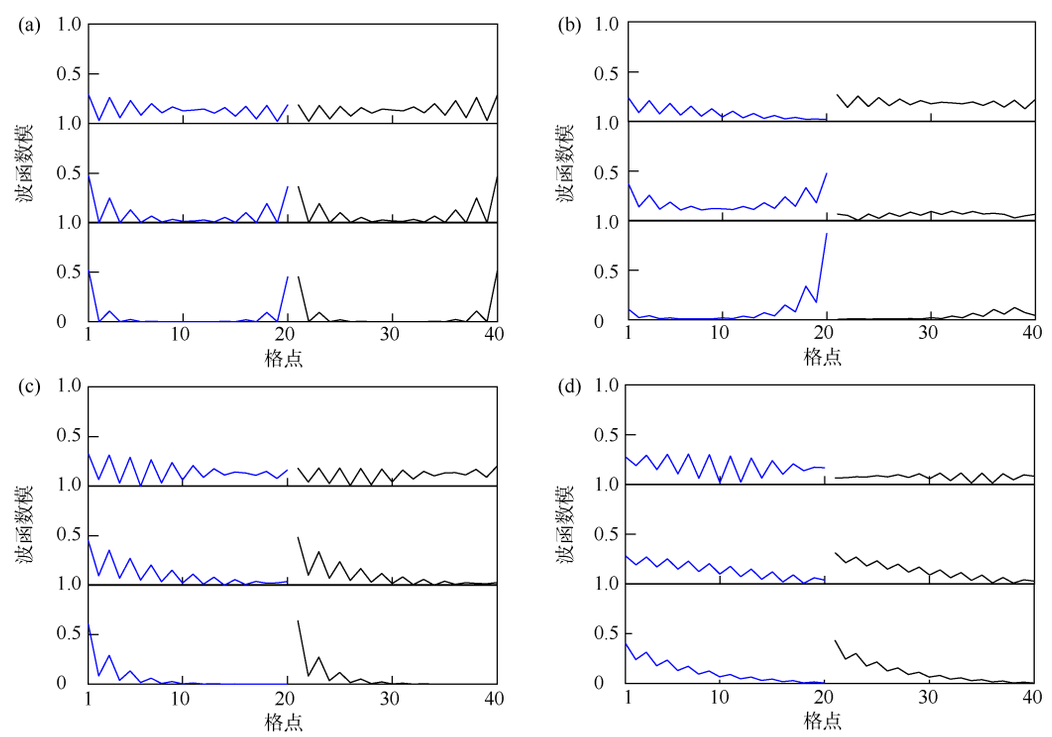


图 6　AB堆叠双层锯齿型石墨烯纳米带的能带结构

(a)无缺陷;(b)$u_{1,A}=u_{1,B}=-0.5$, $u_{2,A}=u_{2,B}=0.5$;(c)$u_{1,A}=u_{2,A}=-0.3$, $u_{1,B}=u_{2,B}=0.3$;(d)$u_{1,A}=u_{2,A}=-0.8$, $u_{1,B}=u_{2,B}=0.8$



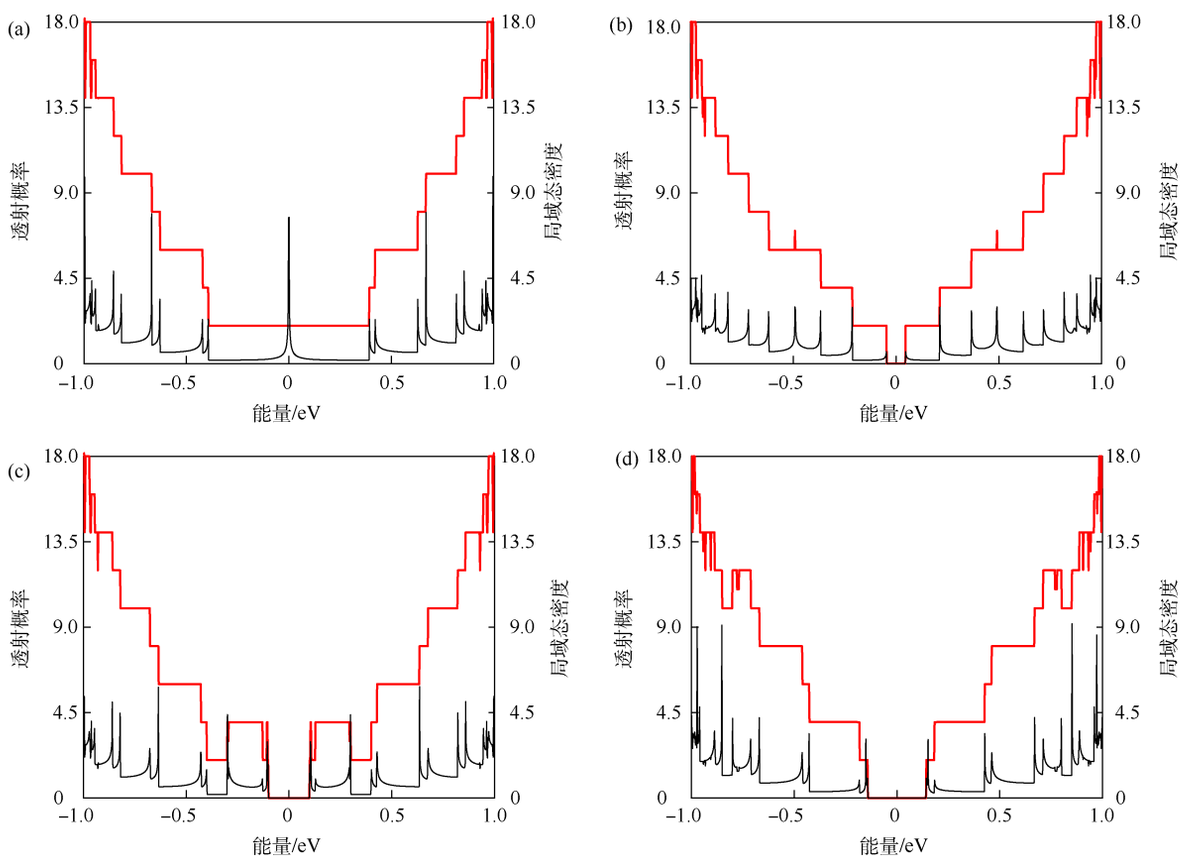
注:蓝色代表上层格点;黑色代表下层格点.

图 7　AB堆叠双层锯齿型石墨烯纳米带导带底单胞格点波函数模随纵向波矢的演化

(a)无缺陷;(b)$u_{1,A}=u_{1,B}=-0.5$, $u_{2,A}=u_{2,B}=0.5$;(c)$u_{1,A}=u_{2,A}=-0.3$, $u_{1,B}=u_{2,B}=0.3$;(d)$u_{1,A}=u_{2,A}=-0.8$, $u_{1,B}=u_{2,B}=0.8$

给出导带底的单胞格点波函数模与波矢k_Y的具体关系,每一种条件展示3个波矢,每幅图中各小图从上到下依次表示波矢k_Y = 0.67π、0.80π和0.90π,X轴为单胞格点位置.当k_Y从0.67π(Dirac点附近)到π时,对于无缺陷情况,电子占据分布较为均匀;随着波矢的增加,当k_Y = 0.80π时,改变边界缺陷的占位能,会使电子占据边态的优势增强,通过研究价带顶的电子占据表明,可以通过改变占位能符号来改变电子在上下层的分布情况;继续增大边界占位能绝对值会使边态占据概率降低,当k_Y = π时,边态占据优势最明显.由此可知,改变边界线缺陷占位能,可以调控电子分布占据边态优势,从而打开单边量子通道,为双层石墨烯半导体元件的应用提供了基础.

AB堆叠双层锯齿型石墨烯纳米带透射概率和局域态密度如图8所示.对于无缺陷情况而言,AB堆叠双层锯齿型石墨烯纳米带在E=0附近的局域态密度也会有尖峰的产生,这依然归因于重合平带的贡献,同样地,可以在透射概率关系图上观察到平台.而改变层间跃迁系数或者同时改变层间跃迁系数和占位能系数时,透射概率和局域态密度在E=0附近的范围内为0,说明此时能够打开一个能隙.



注:红粗实线表示透射概率;黑细实线表示局域态密度.

图8　AB堆叠双层锯齿型石墨烯纳米带透射概率和局域态密度

(a)无缺陷;(b)$u_{1,A} = u_{1,B} = -0.5, u_{2,A} = u_{2,B} = 0.5$;(c)$u_{1,A} = u_{2,A} = -0.3$, $u_{1,B} = u_{2,B} = 0.3$;(d)$u_{1,A} = u_{2,A} = -0.8, u_{1,B} = u_{2,B} = 0.8$

3　结　论

根据单电子紧束缚近似模型,利用有限差分法,本文不仅计算了不同堆叠类型无限长双层锯齿型石墨烯纳米带的能谱及格点波函数,而且计算了两端口双层锯齿型石墨烯纳米带的局域态密度和透射概率,研究了体系上下2条边界子格线缺陷的占位能和层间跃迁积分对纳米带能谱和边态的影响.研究表明:对于AA堆叠,双层上边界A子格和下边界B子格缺陷占位能可调控导带底和价带顶平带色散关系,层间跃迁积分可调控次导带底和次价带顶的平带色散关系,打开体能隙,合适的参数能增大能隙;对于AB堆叠,边缺陷占位能可对费米面周围近乎重合的4条平带产生影响,从而打开一个

能隙,而层间相互作用对平带部分影响不大,无法增大能隙宽度.引入边界线缺陷,对于2种堆叠情况均会增强边态占据优势,打开边界量子通道,且改变占位能的符号可以调控电子分布在上下层的优势,增大占位能的数值会降低边态占据概率.缺陷格点的占位能可通过栅压调控,缺陷格点的层间跃迁可通过应力或衬底调控,这些都为制作新型双层石墨烯纳米器件提供了有力支撑.

参 考 文 献

[1] NOVOSELOV K S, GEIM A K, MOROZOV S V, et al. Electric field effect in atomically thin carbon films[J]. Science, 2004, 306(5696): 666-669.

[2] WAKABAYASHI K, SIGRIST M. Zero-conductance resonances due to flux states in nanographite ribbon junctions[J]. Physical Review Letters, 2000, 84(15): 3390-3393.

[3] BREY L, FERTIG H A. Electronic states of graphene nanoribbons studied with the Dirac equation [J]. Physical Review B, 2006, 73(23): 235411.

[4] MUNOZ-ROJAS F, JACOB D, FERNANDEZ-ROSSIER J, et al. Coherent transport in graphene nanoconstrictions [J]. Physical Review B, 2006, 74(19): 195417.

[5] LEWENKOPF C H, MUCCIOLO E R, NETO A H. Numerical studies of conductivity and Fano factor in disordered graphene[J]. Physical Review B, 2008, 77(8): 081410.

[6] CHEN Z H, LIN Y M, ROOKS M J, et al. Graphenenano-ribbon electronics[J]. Physica E, 2007, 40(2): 228-232.

[7] HAN M Y, OZYILMAZ B, ZHANG Y B, et al. Energy band-gap engineering of graphene nanoribbons [J]. Physical Review Letters, 2007, 98(20): 206805.

[8] WANG X R, OUYANG Y, LI X L, et al. Room temperature all semiconducting sub-10 nm graphene nanoribbon field-effect transistors[J]. Physical Review Letters, 2008, 100(20): 206803.

[9] GUSYNIN V P, SHARAPOV S G. Unconventional integer quantum hall effect in graphene [J]. Physical Review Letters, 2005, 95(14): 146801.

[10] PERES N M R, GUINEA F, NETO A H C. Electronic properties of disordered two-dimensional carbon [J]. Physical Review B, 2006, 73(12): 125411.

[11] KATSNELSON M I, NOVOSELOV K S, GEIM A K. Chiral tunnelling and the Klein paradox in graphene[J]. Nature Physics, 2006, 2(2): 620-625.

[12] MARTINO A D, DELL'ANNA L, EGGER R. Magnetic confinement of massless Dirac fermions in graphene[J]. Physical Review Letters, 2007, 98(6): 066802.

[13] XU H Y, HEINZEL T, EVALDSSON M, et al. Magnetic barriers in graphene nanoribbons: theoretical study of transport properties[J]. Physical Review, 2008, 77(24): 655-664.

[14] MASIR M R, VASILOPOULOS P, MATULIS A, et al. Direction-dependent tunneling through nanostructured magnetic barriers in graphene[J]. Physical Review B, 2008, 77(23): 235443.

[15] FILHO R N, FARIAS G A, PEETERS F M. Graphene ribbons with a line of impurities: opening of a gap[J]. Physical Review B, 2007, 76(19): 193409.

[16] EVALDSSON M, ZOZOULENKO I V, XU H Y, et al. Edge-disorder-induced Anderson localization and conduction gap in graphene nanoribbons[J]. Physical Review B, 2008, 78(16): 161407.

[17] MCCANN E. Asymmetry gap in the electronic band structure of bilayer graphene[J]. Physical Review B, 2006, 74(16): 161403.

[18] KECHEDZHI K, FALKO V I, MCCANN E, et al. Influence of trigonal warping on interference effects in bilayer graphene[J]. Physical Review Letters, 2007, 98(17): 176806.

[19] SNYMAN I, BEENAKKER C W J. Ballistic transmission through a graphene bilayer[J]. Physical Review B, 2007, 75(4): 045322.

[20] ABERGEL D S L, FALKO V I. Optical and magneto-optical far-infrared properties of bilayer graphene[J]. Physical Review B, 2007, 75(15): 155430.

[21] LAI Y H, HO J H, CHANG C P, et al. Magnetoelectronic properties of bilayer Bernal graphene [J]. Physical Review B, 2008, 77(8): 085426.

[22] CASTRO E V, PERES N N R, SANTOS J M B L, et al. Localized states at zigzag edges of bilayer graphene[J]. Physical Review Letters, 2008, 100(2): 026802.

[23] GORBACHEV R V, TIKHONENKO F V, MAYOROV A S, et al. Weak localization in bilayer graphene[J]. Physical Review Letters, 2007, 98(17): 176805.

[24] NILSSON J, NETO A H C, GUINEA F, et al. Electronic properties of bilayer and multilayer graphene [J]. Physical Review B, 2007, 78(4): 045405.

[25] KATSNELSON M I. Minimal conductivity in bilayer graphene[J]. The European Physical Journal B, 2006, 52(2): 151-153.

[26] CSERTI J. Minimal longitudinal dc conductivity of perfect bilayer graphene[J]. Physical Review B, 2007, 75(3): 033405.

[27] WANG L, GAO Y D, WEN B, et al. Fractional fractal quantum Hall effect in graphene superlattices [J]. Science, 2015, 350(6265): 1231-1234.

[28] LI J, WANG K, MCFAUL K J, et al. Gate-controlled topological conducting channels in bilayer graphene[J]. Nature Nanotechnology, 2016, 11(12): 1060-1065.

[29] BITTENCOURT V A S V, BERNARDINI A E. Lattice-layer entanglement in Bernal-stacked bilayer graphene [J]. Physical Review B, 2017, 95(19): 195145.

[30] RUSSO S, OOSTINGA J B, WEHENKEL D, et al. Observation of Aharonov-Bohm conductance oscillations in a graphene ring[J]. Physical Review B, 2008, 77(8): 085413.

[31] CASTRO E V, NOVOSELOV K S, MOROZOV S V, et al. Biased bilayer graphene: semiconductor with a gap tunable by the electric field effect[J]. Physical Review Letters, 2007, 99(21): 216802.

[32] CASTRO E V, PERES N M R, STAUBER T, et al. Low density ferromagnetism in biased bilayer graphene[J]. Physical Review Letters, 2008, 100(18): 186803.

[33] CAO Y, FATEMI V, FANG S A, et al. Unconventional superconductivity in magic-angle graphene superlattices [J]. Nature, 2018, 556(7699): 43-50.

[34] CAO Y, FATEMI V, DEMIR A, et al. Correlated insulator behaviour at half-filling in magic-angle graphene superlattices [J]. Nature, 2018, 55(7699): 80-84.

[35] YANKOWITZ M, CHEN S W, POLSHYN H, et al. Tuning superconductivity in twisted bilayer graphene [J]. Science, 2019, 363(6431): 1059-1064.

[36] NAM N N T, KOSHINO M. Lattice relaxation and energy band modulation in twisted bilayer graphene[J]. Physical Review B, 2017, 96(7): 075311.

[37] TARNOPOLSKY G, KRUCHKOV A J, VISHWANATH A. Origin of magic angles in twisted bilayer graphene [J]. Physical Review Letters, 2019, 122(10): 106405.

[38] IKEDA T N. High-order nonlinear optical response of a twisted bilayer graphene[J]. Physical Review Research, 2020, 2(3): 032015.

[39] KATZ O, REFAEL G, LINDNER N H. Optically induced flat bands in twisted bilayer graphene [J]. Physical Review B, 2020, 102(15): 155123.

[40] KORT-KAMP W J M, CULCHAC F J, CAPAZ R B, et al. Photonic spin Hall effect in bilayer graphene moiré superlattices [J]. Physical Review B, 2018, 98(19): 195431.

[41] SUNKU S S, NI G X, JIANG B Y, et al. Photonic crystals for nano-light in moiré graphene superlattices [J]. Science, 2018, 362(6419): 1153-1156.

[42] POLSHYN H, YANKOWITZ M, CHEN S W, et al. Large linear-in-temperature resistivity in twisted bilayer graphene[J]. Nature Physics, 2019, 15(10): 1011-1016.

[43] ALBORZI M S, RAJABPOUR A, MONTAZERI A. Heat transport in 2D van der Waals heterostructures: an analytical modeling approach [J]. International Journal of Thermal Sciences, 2020, 150(1): 106237.

[44] GONZÁLEZ J, STAUBER T. Kohn-Luttinger superconductivity in twisted bilayer graphene [J]. Physical Review Letters, 2019, 122(2): 026801.

[45] SONG Z D, WANG Z J, SHI W J, et al. All magic angles in twisted bilayer graphene are topological[J]. Physical Review Letters, 2019, 123(3): 036401.

[46] PAL H K, SPITZ S, KINDERMANN M. Emergent geometric frustration and flat band in moiré bilayer graphene[J]. Physical Review Letters, 2018, 123(18): 186402.

[47] JIANG Y H, LAI X Y, WATANABE K, et al. Charge-order and broken rotational symmetry in magic-angle twisted bilayer graphene[J]. Nature, 2019, 573(7772): 91-95.

[48] PARK M J, KIM Y, CHO G Y, et al. Higher-order topological insulator in twisted bilayer graphene [J]. Physical Review Letters, 2019, 123(21): 216803.

[49] ZONDINER U, ROZEN A, RODAN-LEGRAIN D, et al. Cascade of phase transitions and Dirac revivals in magic-angle graphene[J]. Nature, 2020, 582(7811): 203-208.

[50] CAO Y, CHOWDHURY D, RODAN-LEGRAIN D, et al. Strange metal in magic-angle graphene with near Planckian dissipation [J]. Physical Review Letters, 2020, 124(7): 076801.

[51] 丁玉洁.石墨烯纳米带及其复合材料的制备与性能研究[D].哈尔滨:哈尔滨工业大学,2019.

[52] LI X L, WANG X R, ZHANG L, et al. Chemically derived, ultrasmooth graphene nanoribbon semiconductors[J]. Science, 2008, 319(5867): 1229-1232.

[53] KOSYNKIN D V, HIGGINBOTHAM A L, SINITSKII A, et al. Longitudinal unzipping of carbon nanotubes to form graphene nanoribbons [J]. Nature, 2009, 458(7240): 872-877.

[54] DUTTAA S, PATI S. Novel properties of graphene nanoribbons: a review [J]. Journal of Materials Chemistry, 2010, 20(38): 8207-8223.

(下转第45页)

与仿真分析[J].光学精密工程,2008,16(1):71-75.
[2] 赵兴强,温志渝.基于压电材料的振动能量收集器的谐振频率调节[J].压电与声光,2013,35(2):241-244.
[3] WANG H Y, TANG L H, GUO Y, et al. A 2DOF hybrid energy harvester based on combined piezoelectric and electromagnetic conversion mechanisms[J]. Journal of Zhejiang University-Science A (Applied Physics & Engineering),2014,15(9):711-722.
[4] SANG Y J, HUANG X L, LIU H X, et al. A vibration-based hybrid energy harvester for wireless sensor systems[J]. IEEE Transactions on Magnetics, 2012, 48(11):4495-4498.
[5] ABOHAMER M K, AWREJCEWICZ J, STAROSTA R, et al. Influence of the motion of a spring pendulum on energy-harvesting devices[J]. Applied Sciences, 2021, 11(18):2076-3417.
[6] HIBBELER R C. Mechanics of materials [M]. Upper Saddle River: Pearson Prentice Hall Publisher, 2005.
[7] 陈定方,孙科,李立杰,等.微型压电能量收集器的研究现状和发展趋势[J].湖北工业大学学报,2012,27(4):1-8.
[8] 张旭辉,赖正鹏,吴中华,等.新型双稳态压电振动俘能系统的理论建模与实验研究[J].振动工程学报,2019,32(1):87-96.
[9] 袁江波,单小彪,谢涛,等.悬臂梁单晶压电发电机的实验[J].光学精密工程,2009,17(5):1072-1077.
[10] 马小青,李帅波,王喃喃.复合式压电悬臂发电梁设计与实验分析[J].仪表技术与传感器,2019(10):8-11.
[11] 程光明,李新辉,张海滨,等.悬臂式压电双晶片振子夹持长度变化对其动态特性的影响[J].光学精密工程,2014,22(5):1296-1303.
[12] 房立清,张磊.单晶压电悬臂梁等效黏性阻尼建模与实验[J].光学精密工程,2014,22(3):641-648.
[13] 芮小博,李一博,曾周末.压电悬臂梁振动能量收集器研究进展[J].振动与冲击,2020,39(17):112-123.
[14] 关世伟.梁式结构压电:电磁复合俘能技术研究[D].哈尔滨:哈尔滨工业大学,2013.

(责任编辑:兰丽丽)

(上接第32页)

[55] CAI J M, RUFFIEUX P, JAAFAR R, et al. Atomically precise bottom-up fabrication of graphene nanoribbons [J]. Nature, 2010, 466(7305):470-473.
[56] BORRIELLO I, CANTELE G, NINNO D. Graphene nanoribbon electrical decoupling from metallic substrates [J]. Nanoscale, 2013, 5(1):291-298.
[57] JIA X T, HOFMANN M, MEUNIER V, et al. Controlled formation of sharp zigzag and armchair edges in graphitic nanoribbons[J]. Science, 2009, 323(5922): 1701-1705.
[58] JIA X T, CAMPOS-DELGADO J, TERRONES M, et al. Graphene edges: a review of their fabrication and characterization[J]. Nanoscale, 2011, 3(1):86-95.
[59] BERGER C, SONG Z M, LI T B, et al. Ultrathin epitaxial graphite: 2D electron gas properties and a route toward graphene-based nanoelectronics[J]. The Journal of Physical Chemistry B, 2004, 108(52):19912-19916.
[60] EZAWA M. Peculiar width dependence of the electronic properties of carbon nanoribbons[J]. Physical Review B, 2006, 73(4):045432.
[61] ZHANG Z Z, CHANG K, CHAN K S. Resonant tunneling through double-bended graphene nanoribbons [J]. Applied Physics Letters, 2008, 93(6):062106.
[62] WANG Y, YANG S A, QIAN N. Edge states in graphene: from gapped flat-band to gapless chiral modes [J]. Physical Review Letters, 2009, 102(9):096801.
[63] GUNLYCKE D, WHITE C T. Graphene valley filter using a line defect[J]. Physical Review Letters, 2011, 106(13):136806.
[64] XU H Y, HEINZEL T, ZOZOULENKO I V. Edge disorder and localization regimes in bilayer graphene nanoribbons[J]. Physical Review, 2009, 80(4):045308.
[65] 姜鹏程.边界态对双层石墨烯的电导和谷极化的影响[D].石家庄:河北师范大学,2013.
[66] 刘丽丽,龙文.线缺陷对扶手型石墨烯纳米带能隙的调控[J].首都师范大学学报(自然科学版),2016,37(1):20-26+29.
[67] 刘爽,龙文.线缺陷对锯齿型石墨烯带能谱和边态的调控[J].首都师范大学学报(自然科学版),2018,39(1):21-29.

(责任编辑:兰丽丽)